Disorder and the optical spectroscopy of Cr^{3+}-doped glasses. II. Glasses with high and low ligand fields

1991 J. Phys.: Condens. Matter 3 3825

(http://iopscience.iop.org/0953-8984/3/21/015)

J. Phys.: Condens. Matter 3 (1991) 3825–3840. Printed in the UK

Disorder and the optical spectroscopy of Cr^{3+}-doped glasses: II. Glasses with high and low ligand fields

F Rasheed†‡, K P O'Donnell†, B Henderson† and D B Hollis§

† Department of Physics and Applied Physics, University of Strathclyde, Glasgow G4 0NG, UK

§ Department of Physics, Paisley College of Technology, Paisley PA1 2BE, UK

Received 2 November 1990

Abstract. This paper reports spectroscopic studies of Cr^{3+} ions in fluorozirconate, fluoride, borate and telluride glasses in which the average strength of the octahedral crystal field Dq/B varies from 1.6 to 2.4. The emission spectra are shown to be inhomogeneously broadened by disorder. Non-exponential decay of the emission intensity following pulsed excitation is another signature of the extensive disorder in these glasses. The large density of states of two-level systems is shown to account for the larger-than-expected homogeneous width of the R line in lithium borate and potassium borate glasses.

1. Introduction

Recently the present authors (Rasheed *et al* 1991) have discussed the optical properties of a number of Cr^{3+}-doped silicate glasses with compositions chosen to vary the average value of strength of the octahedral crystal field at the Cr^{3+} ion site. The chosen glasses were predominantly low-field glasses for which $^4T_2$ lies below ^2E. In consequence, their emission spectra are expected to consist of broad $^4T_2 \rightarrow {}^4A_2$ bands only. That both R line and $^4T_2 \rightarrow {}^4A_2$ band are observed in some glasses even at 4 K shows that ^2E and $^4T_2$ are close enough together that vibronic mixing of these states occurs in amounts determined by the splitting $\Delta E = E(^2T_2) - E(^2E)$ (Donnelly *et al* 1988, Yamaga *et al* 1989, 1990).

The width of the optical spectra showed that the Cr^{3+} ions occupy a range of sites between which the crystal-field splittings vary. The extensive site-to-site disorder contributes to multi-exponential decay patterns and inhomogeneously broadened R-line and $^4T_2 \rightarrow {}^4A_2$ broad-band spectra. This disorder was studied using narrow-line laser-excited luminescence spectroscopy, luminescence lifetime measurements and time-resolved luminescence spectroscopy applied to both the R line and the $^4T_2 \rightarrow {}^4A_2$ broad band. The nature of the disorder was also probed using fluorescence line narrowing (FLN) to determine the temperature dependence of the homogeneous width of the R line. Such measurements revealed that the excess width of the R line is due to lifetime broadening by interaction with vibrational two-level systems (Bergin *et al* 1986). The present study, involving fluoride, phosphate, borate and tellurite glasses, was undertaken to extend the range of Dq-values experienced by Cr^{3+} ions in vitreous solids.

‡ Permanent address: Department of Physics, Military Engineering Academy, Baghdad, Iraq.

0953-8984/91/213825 + 16 $03.50

Table 1. Compositions of Cr^{3+}-doped glasses.

Glass type	Sample number	Composition (mol%)			
Fluorozirconate		$50ZrF_4$, $4.5AlF_3$,	$20BaF_2$, $0.1CrF_3$	20NaF,	$5.4LaF_3$
Fluoride	G8197	$8.4MgF_2$ $17.0AlF_3$, $2.7Al_2O_3$,	$13.7SrF_2$ $37.6LiF$, $0.05CrF_3$	$5.1BaF_2$, $3.0Al(PO_3)_3$,	$12.5CuF_2$,
Phosphate	G8222	$51.8P_2O_5$, $8.1CaO$,	$10.1ZnO$, $4.8Al_2O_3$,	$25.2Li_2O$, $0.4Cr_2O_3$	
Lithium borate	G8382	$54.4B_2O_3$,	$41.9Li_2O$,	$3.7MgO$,	$0.1Cr_2O_3$
Potassium borate	G8150	$66.5B_2O_3$,	$33.5K_2O$,	$0.05Cr_2O_3$	
Tellurite	G8298	$60.8TeO_2$,	$39.2Na_2O$	$0.05Cr_2O_3$	

2. Experimental techniques

The compositions of the six glasses are given in table 1; they have values of Dq/B that bracket the silicate glasses discussed in the earlier publication (Rasheed *et al* 1991). Both fluoride and fluorozirconate are low-field glasses; the phosphate and borate glasses are very similar to the silicate glasses (Rasheed *et al* 1991) and the tellurite glass is the only high-field glass. The experimental samples were cut and polished to sizes suitable for absorption ($1 \times 5 \times 7$ mm) and fluorescence ($1 \times 2 \times 5$ mm) measurements. Optical absorption measurements were made at 77 K and 300 K in the wavelength range 250–1000 nm using commercial spectrophotometers. Fluorescence due to Cr^{3+} ions was excited using laser radiation from an Ar^+ laser or a dye laser using DCM dye as the active medium. The excitation was chopped at frequencies up to 3 kHz to facilitate the use of phase-sensitive electronics. Spectra were recorded in the wavelength range 650–1200 nm temperatures of 10–300 K achieved using a closed-cycle cryorefrigerator equipped with optical access for exciting and emitted beams. For high-resolution measurements involving the FLN technique, the fluorescence was excited using a single-mode ring dye laser having a spectral bandwidth of about 500 MHz (Rasheed *et al* 1991).

3. Experimental results

3.1. Optical absorption

The measurements of the wavelength dependence of the absorption coefficient of fluoride, phosphate and telluride glasses (figure 1) show the familiar broad absorption bands due to the vibronic $^4A_2 \rightarrow {}^4T_2$ and $^4A_2 \rightarrow {}^4T_1$ transitions. The energy corresponding to the band peaks are quoted in table 2. Also revealed in some cases is a much weaker sharper structure associated with absorption transitions to the ^2E and $^2T_1$ levels. These peak energies may be used to determine the strength of the octahedral crystal field Dq experienced by the Cr^{3+} ions and the electron–electron (Racah) parameters B and C (Sugano *et al* 1970). Although the peak positions are determined by

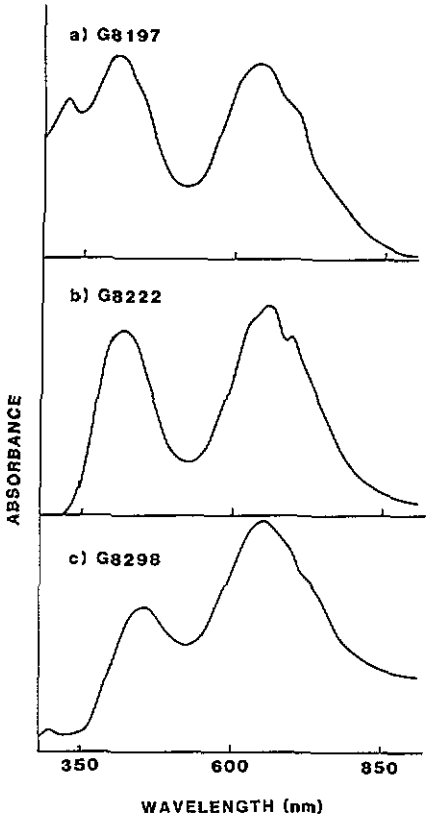

Figure 1. Absorption spectra of Cr^{3+} ions in the wavelength range 300–900 nm for various glasses measured at 300 K: (*a*) fluoride (G8197); (*b*) phosphate (G8222); (*c*) tellurite (G8298).

Table 2. Absorption band positions and level splittings for some Cr^{3+} glasses.

Glass type	^2E (cm^{-1})	$^2T_1$ (cm^{-1})	$^4T_2$ (cm^{-1})	$^4T_1$ (cm^{-1})	B (cm^{-1})	Dq/B	C (cm^{-1})
Fluorozirconate	14 600	15 050	15 300	22 150	850	1.80	2925
Fluoride	14 860	15 530	15 385	23 040	850	1.84	2948
Phosphate	14 660	15 870	15 270	22 370	756	2.02	3073
Lithium borate	14 674	15 570	15 750	23 050	700	2.25	3090
Potassium borate	14 682	15 650	16 085	22 975	710	2.25	3115
Tellurite	14 124	14 925	15 385	21 739	699	2.20	3143

these parameters in the static crystal field, the widths of the $^4A_2 \rightarrow {}^4T_2$, $^4T_1$ bands are normally determined by the strength of the vibronic interaction (Henderson and Imbusch 1989). However, in glasses these bands are inhomogeneously broadened to a significant extent by disorder, in which the Cr^{3+} ions occupy many different octahedral sites in which the splitting parameters are slightly different. For this reason the values of Dq, B and C given in table 2 are averages over the distribution of sites occupied by the Cr^{3+} ions in the various glasses. These results accord with earlier studies of glasses with slightly different compositions (Tischer 1968, Andrews *et al* 1981, Hollis *et al* 1987).

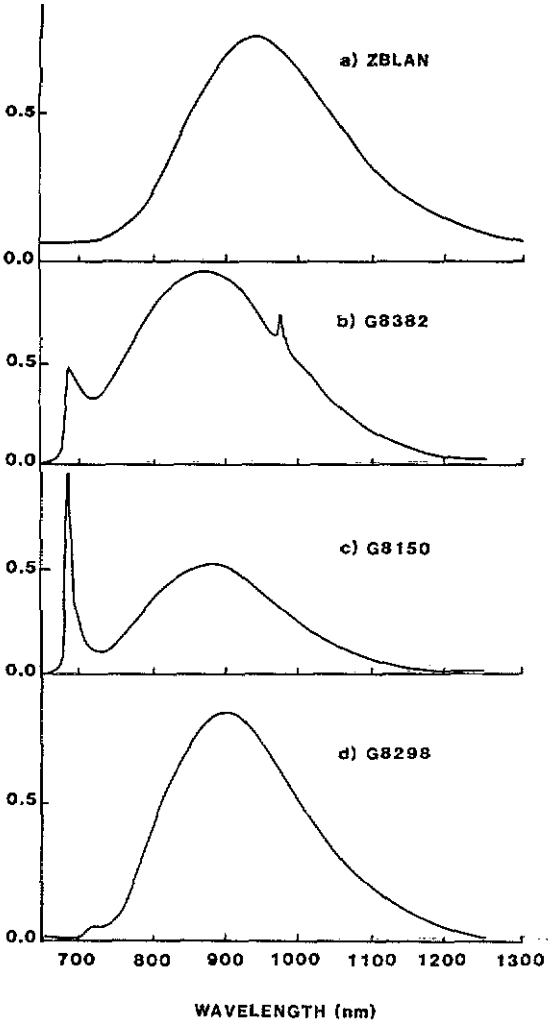

Figure 2. Luminescence spectra of Cr^{3+} ions in various glasses measured at 10 K and excited at 615 nm for (*a*)–(*c*) and using the all-lines output from an Ar^+ laser for (*d*): (*a*) fluorozirconate (ZBLAN); (*b*) lithium borate (G8382); (*c*) potassium borate (G8150); (*d*) tellurite (G8298).

Note that the $^4A_2 \rightarrow {}^2E, {}^2T_1$ transitions in crystals are sharp lines, such that distortions from octahedral symmetry result in distinct splittings. The absence of splittings in glasses also follows from the extensive inhomogeneous broadening that accompanies disorder in vitreous solids. In consequence, since non-cubic distortions have not been included in the analysis of the energy level structure, the average values of Dq, B and C are only approximate.

3.2. Steady-state luminescence

The emission spectra of fluorozirconate, lithium and potassium borate and tellurite glasses are shown in figure 2. There is no detectable R-line emission ($^2E \rightarrow {}^4A_2$) for the fluorozirconate glasses; only the broad-band $^4T_2 \rightarrow {}^4A_2$ emission is detected. These are clearly low-field materials in which the $^4T_2$ level is lower in energy than the ^2E level for all sites. The fluoride glass (G8197) and the phosphate glass (G8022) also behave as low-field hosts for Cr^{3+} ions. In contrast, the lithium borate glass (G8382), the potassium

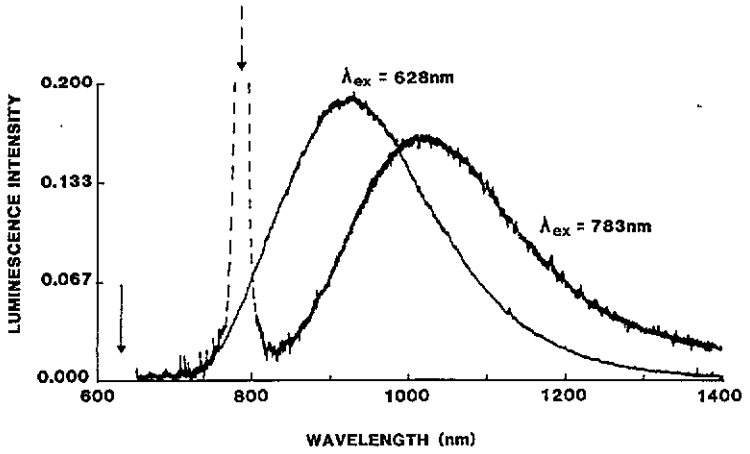

Figure 3. Comparison of the luminescence spectrum of Cr^{3+} in fluorozirconate glass (ZBLAN) excited at two excitation wavelengths: (*a*) 628 nm; (*b*) 783 nm.

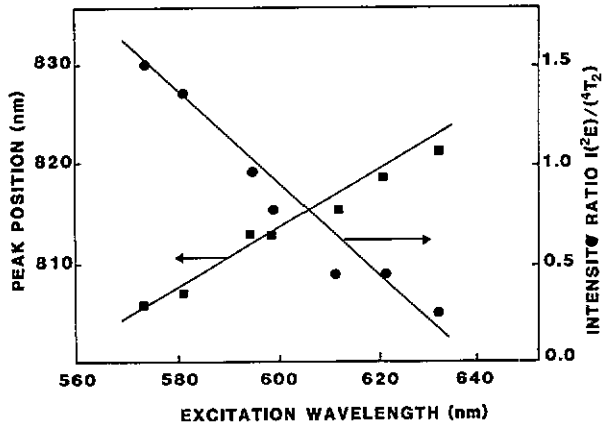

Figure 4. The dependence of the $^4T_2 \rightarrow {}^4A_2$ emission band peak wavelength and intensity ratio $I(^2E)/I(^4T_2)$ on the excitation wavelength for potassium borate glass (G8150) measured at $T = 10$ K.

borate glass (G8150) and the tellurite glass (G8298) have emission spectra that contain both the R line and the $^4T_2 \rightarrow {}^4A_2$ band in different proportions. These are *representative* luminescence spectra since the relative intensities of the R line and broad band and the peak wavelength of the $^4T_2 \rightarrow {}^4A_2$ emission band are sensitive to the excitation wavelength. The shift in the $^4T_2 \rightarrow {}^4A_2$ emission band in the fluorozirconate glass is shown in figure 3. In the potassium borate glass, as figure 4 shows, the peak wavelength of the $^4T_2 \rightarrow {}^4A_2$ band increases linearly with increasing excitation wavelength whereas the intensity ratio $R = I(^2E)/I(^4T_2)$ decreases linearly over the same range of wavelengths. Essentially the narrow-band laser selects Cr^{3+} ions occupying a very small range of Dq-values. Hence figure 4 represents the variation in optical properties with varying Dq. Related data are shown in figure 5 where the band centroid and intensity ratio R

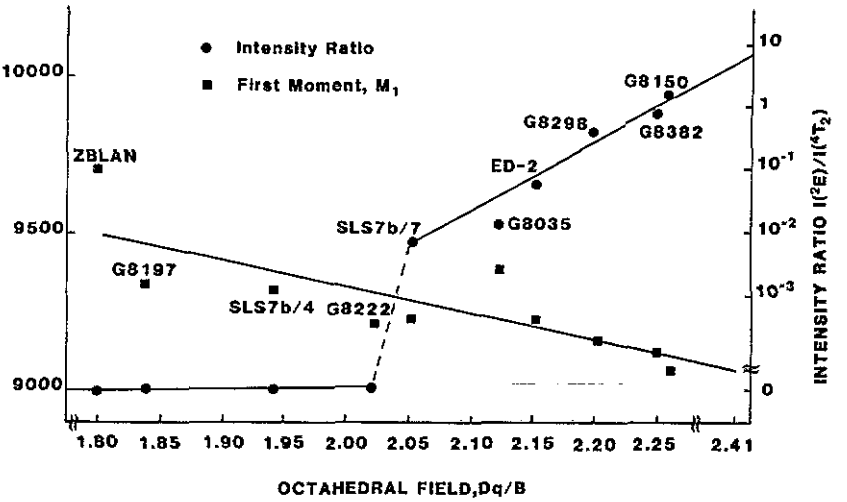

Figure 5. Variations in the band centroid of the $^4T_2 \rightarrow {}^4A_2$ band and intensity ratio $R = I(^2E)/I(^4T_2)$ plotted as a function of Dq/B. The luminescence was excited at the peak of the $^4T_2 \rightarrow {}^4A_2$ absorption band at $T = 10$ K. (Data for a range of silicate glasses are included for comparison (Rasheed *et al* 1991).)

Table 3. Relative intensities of the Cr^{3+} emission in various glasses at 10 and 300 K.

Glass type	Sample number	I(300 K)	I(10 K)	I(300 K)/I(10 K)
Silicate	G8035	2.36	8.3	0.28
Fluoride	G8197	0.27	1.97	0.14
Lithium borate	G8382	0.15	1.32	0.11
Fluorozirconate	ZBLAN	0.02	1.41	0.014

are plotted as functions of the mean value of Dq for different glasses including the silicate glasses discussed in the earlier publication (Rasheed *et al* 1991). In such glasses the integrated intensity over the whole band shape is strongly temperature dependent (table 3). Although at low temperatures the quantum efficiency is about 30% relative to for example $Al_2O_3:Cr^{3+}$, as figure 6 shows the luminescence output decreases further by a factor of 20–30 between $T = 10$ and 300 K.

3.3. Time-resolved spectroscopy

The luminescence decay patterns after pulsed excitation are not simple exponential decreases in intensity with time. Both R-line and broad-band processes are non-exponential, a clear signature of disorder in the glassy structure (Johnscher 1986). Generally the R-line emission decays more slowly by a factor of 10 or so than the $^4T_2 \rightarrow {}^4A_2$ broad band. These differences in decay rates facilitate the time resolution of overlapping components in the luminescence spectrum. The example shown in figure 7 is for the potassium borate glass (G8150). In using the technique of phase-sensitive

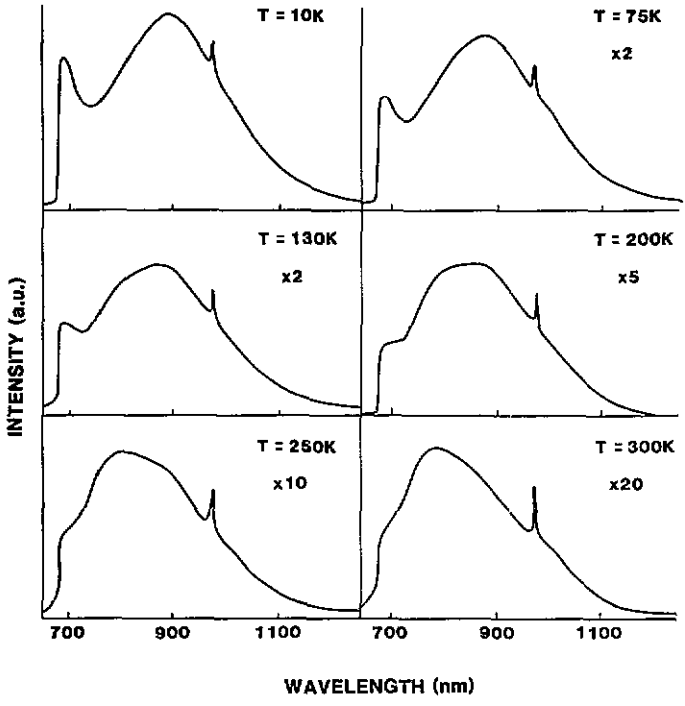

Figure 6. Temperature dependence of the emission spectrum of Cr^{3+} ions in lithium borate glass (G8382).

detection (Engstrom and Mollenauer 1975) the phase control of the lock-in detector is adjusted to reduce the signal to zero at the R-line or broad-band peak, so permitting the presentation of either signal alone. Accompanying the resolved R line is the very weak vibrational sideband in the wavelength region 693–730 nm.

In similar measurements on the lithium borate glass, in which the R line is much broader than in the other glasses, it was not possible to zero the intensity completely in the R-line region because of two components with rather similar lifetimes. Time-resolved measurements of Cr^{3+}-doped lithium borate glass were made using a box-car integrator connected at the output of the photomultiplier tube, and a series of spectra recorded for various delay periods following excitation. After a delay of 2 ms the fast $^4T_2 \rightarrow {}^4A_2$ emission has completely decayed and only the $^2E \rightarrow {}^4A_2$ peak is observed. Measurements after very long decay times were made using very slow chopper speeds (5 Hz) and high amplifier gain. Delay times exceeding 5 ms result in broadening of the ^2E emission (figure 8) which is revealed after 13 ms decay as due to two components in the R line at 684 and 706 nm.

3.4. Fluorescence line narrowing

In figure 9 is shown the R line of Cr^{3+} ions in the potassium borate glass excited at $\lambda =$ 655 nm and measured at a low temperature ($T = 10$ K). An example of the FLN spectrum excited within the R-line shape at $\lambda = 682.9$ nm is also shown. Since the width of the FLN spectrum (about 1 cm^{-1}) is comparable with the homogeneous width, it is evident from

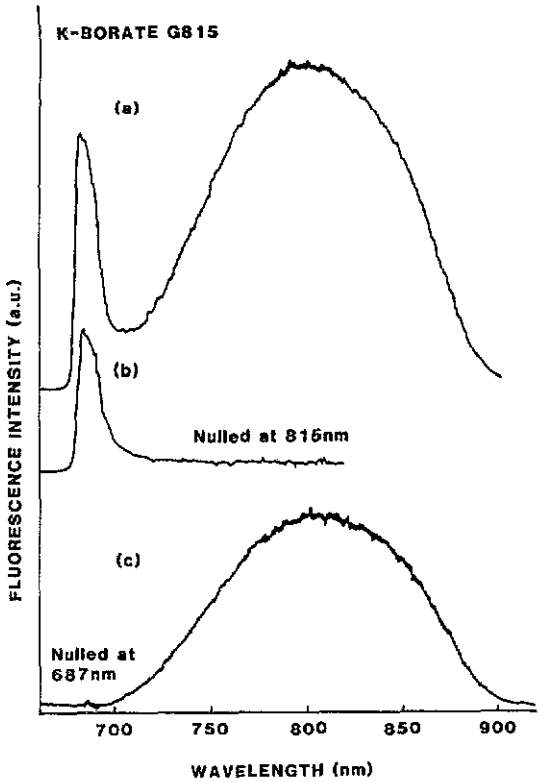

Figure 7. Time-resolved R line and $^4T_2 \rightarrow {}^4A_2$ band from Cr^{3+} ions in potassium glass (G8150) measured at 10 K using phase-sensitive detection.

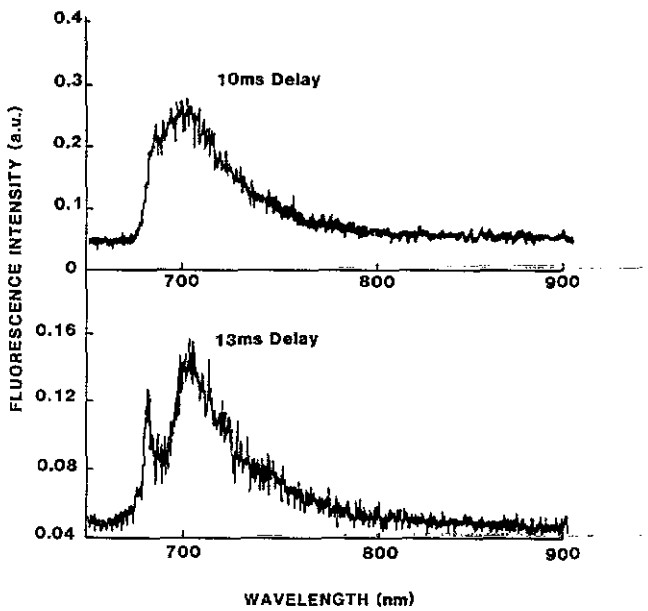

Figure 8. Time-resolved components for the R line from Cr^{3+} ions in lithium borate glass (G8382) measured at 10 K using box car integration.

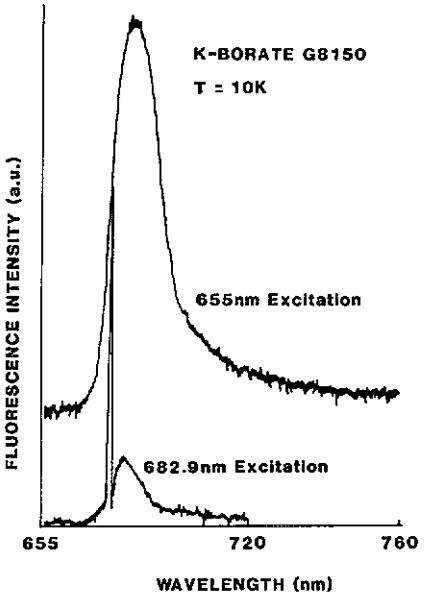

Figure 9. FLN spectrum in the R line of Cr^{3+} ions in potassium borate glass (G8150) measured at $T = 10$ K compared with the R line measured at the same temperature.

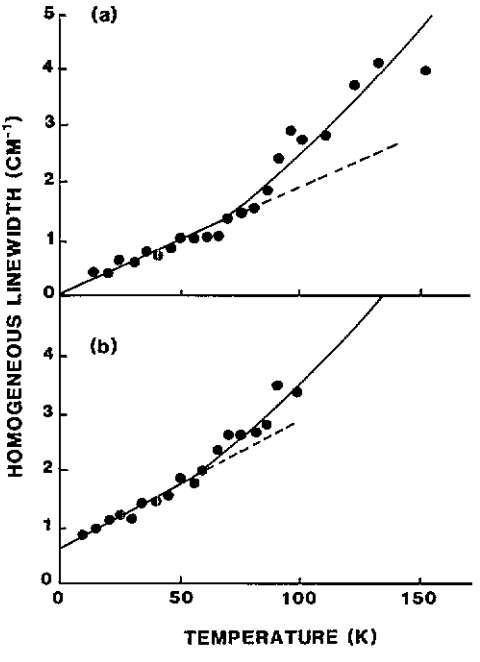

Figure 10. Temperature dependence of the homogeneous width $\Gamma_h(T)$ for the resonant FLN R line of Cr^{3+} ions in lithium borate glass (G8382) and potassium borate glass (G8150).

the normal width of the R line which is about 200 cm^{-1} that the disorder in this glass is very extensive. This result is typical of glasses which emit the R line (lithium borate (G8382) and tellurite (G8298)). Similar results have been reported for silicate glasses (Bergin *et al* 1986, Rasheed *et al* 1991).

Also evident in the FLN spectrum (figure 9) is the rather broader R_1 line excited non-resonantly by the laser line at $\lambda = 682.9$ nm. On the assumption of an octahedral arrangement of ligand ions undergoing tetragonal distortions, the ^2E state splits into ^2Eu and ^2Ev levels with ^2Eu at the higher energy. If at low temperatures the laser line resonantly excites some ions to the ^2Eu level (i.e. the R_1 line), they will decay non-radiatively to the ^2Ev level, emitting the R_1 line. As the laser lines is tuned over the wavelength range of the inhomogeneously broadened R line, the R_1 component shifts linearly to longer wavelengths. The splitting of the ^2E level, measured as the energy difference between the resonant (R_2) and non-resonant (R_1) components in the FLN spectrum is 52 cm^{-1} at $\lambda = 678$ nm, increasing linearly to 60 cm^{-1} at 690 nm. At a higher temperature ($T = 77$ K), one detects also an R_2 component on the short-wavelength side of the resonant FLN signal. The laser line excites resonantly the ^2Ev level of some Cr^{3+} ions which are thermally excited up to the ^2Eu level, which emits the R_2 component via $^2Eu \rightarrow {}^4A_2$ transitions. For the lithium borate glass the ^2E-state splitting is observed to be 87 cm^{-1} using an excitation wavelength of 676.5 nm, increasing to 105 cm^{-1} for excitation at $\lambda = 691$ cm^{-1}.

The measured lineshape is a convolution of the system lineshape (including laser line) and the homogeneous broadening of the $^2E \rightarrow {}^4A_2$ transition (Kushida and Takushi

1975), assuming that the ground state-splitting is negligible (Imbusch and Boulon 1987). The system linewidth, assumed to be Gaussian, is important at low temperatures. At higher temperatures, homogeneous broadening is dominant and the detected spectrum is Lorentzian. Deconvolution of the detected linewidth into a homogeneous and a system linewidth is required to measure the temperature dependence of the homogeneous broadening. The technique of Wertheim *et al* (1974), which uses standard curves for deconvoluting the composite lineshape was adopted (Rasheed 1988), from which the homogeneous width can be evaluated from the measured linewidth and the laser linewidth. The relationship between the detected linewidth $\Gamma(T)$, the laser linewidth Γ_L and the homogeneous linewidth $\Gamma_h(T)$ is often written as (Kushida and Takushi 1975)

$$\Gamma(T) = \Gamma_L + 2\Gamma_h(T). \tag{1}$$

Values of $\Gamma_h(T)$ measured for both lithium borate and potassium borate glasses following this procedure are plotted in figure 10 for the temperature range 10–150 K. The general trends are similar to those reported for silicate glasses (Bergin *et al* 1986, Rasheed *et al* 1991), although the homogeneous widths of the borate glasses exceed those of the silicate glasses. At low temperatures, $\Gamma_h(T)$ increases linearly with increasing temperature; a transition from linear to quadratic dependence on T occurs at different temperatures in the two glasses.

4. Discussion

4.1. General spectral features

Usually the optical properties of Cr^{3+} ions are discussed in terms of the Tanabe–Sugano diagram, in which the energy levels E/B are plotted as a function of the octahedral field strength Dq/B for constant values of C/B. The interelectron interaction (or Racah) parameters B and C should not depend strongly on the host. The major feature revealed in the Tanabe–Sugano diagram related to the present discussion is the relative positions of the $^4T_2$ and ^2E levels. For $Dq/B < 2.2$ (low-field sites) the $^4T_2$ level lies below ^2E in energy whereas for $Dq/B > 2.2$ (high-field sites) the obverse obtains. This ordering of levels determines the shape of the luminescence spectrum. In crystalline solids such as Cr^{3+}-doped $KZnF_3$, where Dq/B is about 1.8, $^4T_2$ is lowest and a broad near-infrared luminescence band is observed owing to parity-forbidden $^4T_2 \rightarrow {}^4A_2$ transitions with a radiative lifetime of about 100 μs. For Al_2O_3, where $Dq/B \simeq 2.8$, the emission is in the form of the sharp R line and its vibronic sideband with a radiative lifetime of about 3.4 ms. In contrast, garnets such as $Gd_3Sc_2Ga_3O_{12}$ and $Gd_3Sc_2Al_3O_{12}$ provide octahedral field strengths near the ^2E–$^4T_2$ crossing point (Boulon *et al* 1988, Donnelly *et al* 1989, Yamaga *et al* 1989, 1990, Struve and Huber 1985). The combined effects of spin–orbit and electron–phonon couplings then admix the ^2E and $^4T_2$ levels. Since the emitting level is neither 'pure' ^2E nor 'pure' $^4T_2$, the emission spectrum is an admixture of the R line and $^4T_2 \rightarrow {}^4A_2$ vibronic broad band. This then defines an intermediate octahedral field region, $2.1 < Dq < 2.3$, separating the low-field and high-field regions.

The fluoride glass (G8197), the fluorozirconate glass (FZBLAN) and the phosphate glass provide exclusively low-field sites for Cr^{3+} ions. The intensity ratios $R = I(^2E)/I(^4T_2)$ for these glasses and for the silicate glass (SLS7b/4) are essentially zero (figure 5). The borate glasses (G8382 and G8150) and the tellurite glass (G8298) are at

the high-field extreme of the intermediate-field range, and the emission spectrum is a composite of the R line and $^4T_2 \rightarrow {}^4A_2$ broad band. The other silicate glasses (SLS7b/7, G8035 and ED-2) are also examples of intermediate crystal-field sites. For the six glasses shown in figure 4 with average values of Dq/B exceeding 2.05 the relative intensity $I(^2E)/I(^4T_2)$ increases with increasing Dq/B until the two emission processes make approximately equal contributions to the total intensity. Apparently, none of the glasses studied is a true high-field glass. If such were the case, only the R-line emission would be observed.

The simple crystal-field interpretation of the spectra must be modified to include effects due to inhomogeneous broadening by disorder. Such effects are revealed most clearly in the FLN studies of the R line (figure 9). However, as figure 3 shows for the fluoride glass, even the broad $^4T_2 \rightarrow {}^4A_2$ bands are significantly broadened by the range of Dq-values provided by the different sites occupied by the Cr^{3+} ions. Varying the excitation wavelength from 628 to 783 nm shifts the entire intensity distribution into the infrared by some 100 nm. The effect is shown in greater detail in figure 4 for the potassium borate glass (G8150); shorter wavelengths excite predominantly sites with larger values of Dq/B, which have larger splittings ΔE between the $^4T_2$ and ^2E levels. At longer excitation wavelengths, ions occupying sites with smaller values of Dq are excited and in consequence the peak shifts to longer wavelengths also. There is a concomitant decrease in $I(^2E)/I(^4T_2)$. The width of the R line in these materials (200–250 cm^{-1}) suggests that crystal-field strengths correspond to a range of ± 0.06 in Dq/B about the average value calculated from the positions of the band peaks. As noted above, in the intermediate-field region, the wavefunction admixture determines the optical band shape and the admixture coefficients involve ΔE as energy denominators (Healy *et al* 1989, Yamaga *et al* 1989, 1990). A quantitative description of the spectral variations with an average value of Dq/B is obviously complex; nevertheless the trends in figure 5 are clearly in the correct sense. The apparent discontinuity in figure 5 at $Dq/B \simeq 2.05$ indicates that below this value the glasses tend to provide only low-field sites.

The wide range of glasses that we have studied (e.g. see figure 5) all provide approximately octahedral ligand-field environments for Cr^{3+} impurity ions. Table 4 lists values of Dq/B together with estimated values of molar density of oxygen and the molar concentration of glass former ions for these glasses. (In constructing table 4 the molar volume of O^{2-} is assumed to be twice that of F^- and the effect of covalency in such as Si—O, P—O and B—O bonds has been ignored.) A number of general trends are apparent, although the potassium borate glass (G8150) and the sodium tellurite glass (G8298) are somewhat anomalous. Nevertheless, the anion packing density varies with glass former, decreasing along the series borate → phosphate → silicate → fluoride. Furthermore, larger modifier ions ($K^+ > Na^+ > Li^+$) provide for a lower oxygen content in the glasses. Changing the percentage of the modifier ion has a smaller effect than changing the type of modifier ion has. Finally, changing the anion type is important, F^- producing a lower effective electron density than O^{2-} does. As is anticipated, the higher anion packing density is reflected in the largest values of Dq/B, the fluorides providing only weak-field sites for the Cr^{3+} impurity. We have no explanation for the apparently anomalous behaviour of the potassium borate and sodium tellurite glasses.

4.2. Radiative versus non-radiative decay

The substantial width of the $^4T_2 \rightarrow {}^4A_2$ luminescence band suggests potential application as broad band tunable solid state lasers. The half-width in figure 3 is of order 250 nm.

Table 4. Octahedral crystal field, anion packing density and molecular amount of modifier in various glasses. The anion packing densities are estimated from the compositions ([1] and table 1) and known densities.

Glass type	Sample number	Anion packing density (mol cm^{-3})	Amount of modifier (mol%)	Octahedral field Dq/B	Reference
Sodium barium fluorozirconate	ZBLAN	0.055	60	1.80	
Lithium tin fluoride	G8197	0.043	34	1.84	Comyns (1990)
Sodium tellurite	G8298	0.054	60	2.20	Mazarin *et al* (1985, p 674)
Potassium lead silicate	SLS7b/4	0.068	74	1.95	
Potassium borate	G8150	0.069	66	2.25	Mazarin *et al* (1985, p 83)
Sodium calcium silicate	SLS7b/7	0.072	70	2.05	
Lithium calcium silicate	ED-2	0.075	62	2.15	Paul (1982)
Lithium calcium silicate	G8035	0.077	69	2.10	Paul (1982)
Lithium zinc phosphate	G8222	0.079	55	2.05	Mazarin *et al* (1985, pp 470, 520)
Lithium borate	G8382	0.093	54	2.25	Mazarin *et al* (1985, p 85)

Unfortunately, non-radiative decay militates against laser action at least at 300 K. This is illustrated in table 3, which compares the relative intensities at 10 and 300 K for four different glasses. Obviously the fluorozirconate glass is particularly adversely affected by non-radiative decay at the higher temperature. These variations, and those illustrated in figure 6 for the lithium borate glass (G8382) are due to luminescence quenching as a consequence of the overlap between the configurational coordinate curves of the $^4T_2$ and $^4A_2$ states. Essentially the activation energy for thermally assisted non-radiative decay is just the energy separation between the lowest point in the configurational coordinate curve for the $^4T_2$ state and the crossover point for the $^4T_2$ and $^4A_2$ states. If the particular crystal field makes the $^4T_2$-state parabola shallower, then this activation energy is reduced. Such is the case in fluoride-containing glasses (table 3) because of the weaker ligand fields. However, more generally the $^4T_2 \rightarrow {}^4A_2$ band is vibronically induced, i.e. for a transition between even-parity states there must be a promoting vibrational mode of the appropriate odd-parity symmetry. This restriction applies to both radiative and non-radiative transitions. In glasses, where there is an absence of long-range symmetry, the $^4T_2 \rightarrow {}^4A_2$ mixing will take place by static asymmetries in the crystal field confirmed as present in glasses by the inhomogeneous broadening of the optical transitions.

One further consequence of the disorder is the multi-exponential or non-exponential decay patterns. The different scales of the decay patterns makes resolution of the different spectral components possible (see, e.g., figures 7 and 8). Irrespective of the time resolution of the R line and broad band the observations of decay patterns which are not single exponential is a clear signature of disorder. The resolution of the emission spectrum out of the ^2E and $^4T_2$ states is particularly clear in figure 7. Nevertheless both the R line ($^4E_2 \rightarrow {}^4A_2$) and the broad band ($^4T_2 \rightarrow {}^4A_2$) are very much broader than in crystalline materials. The identification of two R-line processes in lithium borate glasses using time-resolved techniques is intriguing. If the Cr^{3+} concentration was high, then Cr–Cr pairs might be anticipated to provide additional spectral components. The fact that as little as 0.01 wt% Cr_2O_3 is present in the lithium borate glass suggest that pair lines are most unlikely. Instead it seems probable that Li^+–O^{2-}–Cr^{3+} clusters form, which have slightly different energies from the normal Cr^{3+}–O^{2-} octahedral arrangements.

Unfortunately it is difficult to distinguish between decay patterns that are multi-exponential and non-exponential. If the emitting centres are discrete, i.e. they do not interact, then multi-exponential decays are anticipated (see, e.g., Boulon *et al* 1988). For the discrete centres in glasses, it is not possible to resolve the individual exponential decays. In contrast, if the relaxation process takes place in disordered solids, then the decay is intrinsically non-exponential if the relaxing centres interact via many-body interactions. For a system of interacting centres the differential equation governing the return to equilibrium after pulsed excitation is

$$\frac{dI_i(t)}{dt} = -\gamma_i I_i(t) - \sum_j I_i(t) I_j(t) V_{ij} \tag{2}$$

where γ_i is the decay coefficient and V_{ij} is the coupling between excitations at sites i and j (Huber 1984, Jonscher 1986). If $V_{ij} = 0$, the solution to equation (2) is exponential in time. However, with the summation term present, the solution to equation (2) is necessarily non-exponential. In glasses, optical centres experience a range of potential wells and are coupled via electric dipole–dipole interactions of the tunnelling modes of two-level systems.

4.3. Homogeneous broadening of the R line

The significance of the two-level systems may be determined from the temperature dependence of the homogeneous width of the R line. Such measurements (figure 10) in comparison with similar measurements on the R line in single crystals such as Al_2O_3 reveal an excess homogeneous width in glasses. This excess width arises from the interaction of the Cr^{3+} electronic levels with local ligand motions, which vibrate in double-well potentials with minima very close together in energy. The atoms may then tunnel between the two potential wells. Such excitations have rather low energies (about 1 cm^{-1}) and rather high densities of states. In deriving the density of vibrational excitations from the homogeneous width, Bergin *et al* (1986) used an amplitude model to describe the electron–vibrational coupling. The density-of-states function $\rho(\omega)$ is proportional to $\omega I(\omega)$ and may be determined from the shape of the R-line sideband i.e. intensity $I(\omega)$. From the experimental $I(\omega)$ it is possible to show that, for the potassium borate glass, $\rho(\omega) = \alpha\omega^2$ for $0 < \omega < 50\ cm^{-1}$ and $\rho(\omega) = 2\alpha\omega_1^2$ in the range $\omega_1 < \omega < 350\ cm^{-1}$ (Rasheed 1988). For a Debye crystal, where the strain model of the electron–vibrational interaction is more appropriate (Henderson and Imbusch 1989), the corresponding density-of-states function may be expressed as $\rho(\omega) = \beta\omega^2$ for $0 < \omega < 350\ cm^{-1}$ (McCumber and Sturge 1963). By assuming equal numbers of vibrational modes per unit volume of glass and of crystal, i.e.

$$\int^{\infty} [\rho(\omega)\,d\omega]_{\text{crystals}} = \int^{\infty} [\rho(\omega)\,d\omega]_{\text{glass}}$$

we determine that the constants in the density-of-states functions are in the ratio $\alpha/\beta \simeq 54$ for the potassium borate glass.

The Huang–Rhys factor, determined from the relative integrated intensities of the zero-phonon line and the sideband, is $S \simeq 1$ for ruby and about 6 for the potassium borate glass. Hence we may write

$$\int_0^{\infty} I^{c}(\omega)\,d\omega = 6\int_0^{\infty} I^{g}(\omega)\,d\omega.$$

On substituting the appropriate expressions for $I(\omega)$ for glass (amplitude model) and crystals (strain model) we determine from the experimental results that the ratio of the constants of integration, the so-called electronic sensitivity factors $F^{c}/F^{g} = 0.6v^2/\omega_1^2$, where v is the average velocity of sound in the crystal. Utilizing the expression for the homogeneous linewidth due to Raman relaxation appropriate to high-temperature behaviour and taking ratios for the linewidth of temperature T for crystal and glass yield

$$\frac{\Gamma^{c}(80)}{\Gamma^{g}(80)} = 0.021$$

using the experimental values for α/β and F^{c}/F^{g}. For the potassium borate glass, the value of $\Gamma(T)$ at 80 K is 2.8 cm^{-1} and, for ruby at the same temperature, $\Gamma(T)$ is 0.17 cm^{-1} so that this ratio is 0.065. The fact that the observed and calculated ratios are of the same order of magnitude, bearing in mind the assumptions made in the model calculations, is reassuring and strengthens the conclusion that the high-temperature broadening process involves Raman relaxation.

5. Conclusions

The results presented here are for glassy materials that bracket the ranges for the Dq experienced by Cr^{3+} ions in silicate glasses. Both fluoride and fluorozirconate glasses provide weak-field sites only and luminescence is observed only a broad $^4T_2 \rightarrow {}^4A_2$ band. The borate and tellurite glasses provide higher-field sites so that the luminescence spectrum reveals both R-line and broad-band processes. Although the quantum efficiency is reasonably high at low temperatures (about 30%), it is reduced to between 1% (fluorozirconate) and 15% (fluoride) at 300 K. Thus these glasses are unsuitable for solid state laser action at room temperature.

Both broad-band and R-line spectra are inhomogeneously broadened by disorder. This inhomogeneous broadening leads to interesting variations in band shape depending upon excitation wavelength. Disorder also leads to multi-exponent or non-exponential luminescence decay patterns following pulsed excitation. The homogeneous width of the R-line transition is also influenced by vibrational disorder associated with electronic coupling to the tunnelling modes of two-level systems. By using an amplitude model of the electron–vibrational interaction, reasonable estimates may be made of the homogeneous width in the high-temperature region assuming relaxation via the Raman process.

Acknowledgments

At Strathclyde this work has been supported by a Research Grant (GR/E/32549) under the Science and Engineering Research Council–Ministry of Defence scheme. The fluorozirconate glass was prepared by Dr A Clare at the University of Sheffield, where the work was supported by research contract RU10-40 from the Procurement Division of the Ministry of Defence.

References

Andrews L J, Lempicki A and McCallum B C 1981 *J. Phys. Chem.* **74** 556

Bergin F, Donegan J F, Glynn T J and Imbusch G F 1986 *J. Lumin.* **34** 307

Boulon G, Garapon C and Monteil A 1988 *Excited States of Transition Metal Ions* ed W Jezowska-Trzebiatowska, J Legendziewicz and W Strek (Singapore: World Scientific) p 96

Comyns A E (ed) 1990 *Crit. Rep. Appl. Chem.* **27** table 6.3

Donnelly C T, Healy S M, Glynn T J, Imbusch G F and Morgan G P 1988 *J. Lumin.* **42** 119

Engstrom H and Mollenauer L F 1975 *Phys. Rev.* B 7 1616

Henderson B and Imbusch G F 1989 *Optical Spectroscopy of Inorganic Solids* (Oxford: Oxford University Press)

Hollis D B, Parke S and Payne M J 1987 *Solid State Lasers II (Springer Series in Optical Science 52)* ed L G de Shazer, A B Budgor and A Pinto (Berlin: Springer) pp 53–61

Huber D L 1984 *Coherence and Energy Transfer in Glasses* ed P A Fleury and B Golding (New York: Plenum) p 125

Imbusch G F and Boulon G 1987 *Phys. Scr.* **T19** 354

Jonscher A K 1986 *Structure and Bonding in Non-crystalline Solids* ed G E Walrafen and A G Revesz (New York: Plenum) p 101

Kushida T and Takushi E 1975 *Phys. Rev.* B **12** 824

Mazarin O V, Streltsina M V and Shvaiko-Shvaikovskaya T P 1985 *Handbook of Glass Data part B: Single Component and Binary Non-silicate Oxide Glasses (Physical Sciences Series 15)* (Oxford: Elsevier)

McCumber D E and Sturge M D 1963 *J. Appl. Phys.* **34** 1682

Paul A 1982 *Chemistry of Glasses* (London: Chapman and Hall) p 66
Rasheed F F 1988 *PhD Thesis* University of Strathclyde
Rasheed F F, O'Donnell K P, Henderson B and Hollis D B 1991 *J. Phys.: Condens. Matter* **3** 1915
Struve B and Huber G 1985 *Appl. Phys.* B **57** 45
Sugano S, Tanabe Y and Kamimura H 1970 *Multiplets of Transition Metal Ions in Crystals* (New York: Academic)
Tischer R E 1968 *J. Chem. Phys.* **48** 4291
Wertheim G K, Butler M A, West K W and Buchanan D N F 1974 *Rev. Sci. Instrum.* **14** 1369
Yamaga M, Henderson B and O'Donnell K P 1989 *J. Phys.: Condens. Matter* **1** 9175
Yamaga M, Henderson B, O'Donnell K P, Tager-Cowan C and Marshall A 1990 *Appl. Phys.* B **50** 425